ucture/distribution
stems

OMINIC L. BOCCELLI,
CHELL J. SMALL,
D URMILA M. DIWEKAR

The removal of particulate matter is central to the drinking water treatment process. An integrated model for describing contact, direct, and nonsweep conventional filtration is incorporated into an optimization framework to determine least-cost treatment configurations and design parameters that satisfy hydraulic and effluent concentration constraints. Various influent particle concentrations, size distributions, and size ranges under different flow rates and particle densities are explored to illustrate the importance of size distribution characteristics, flow rate, and particle density on design decisions. In general, contact filtration and conventional filtration are the predominant treatment processes, with direct filtration used sparingly for waters with higher concentrations of small particles. The results illustrate that the volume average diameter is not sufficient to characterize the treatment performance; rather, the particle size range and distribution shape are also needed to determine the appropriate treatment configuration. Increasing the design flow rate (2, 10, and 75 mgd [7.57, 37.85, and 283.88 ML/d]) and particle density (1.05, 1.20, and 2.40 g/cm$^3$) both lead to a preference for contact filtration over conventional filtration.

# Treatment plant design for particulate removal:

## EFFECTS OF FLOW RATE AND PARTICLE CHARACTERISTICS

One of the fundamental goals of drinking water treatment is the removal of particulate matter from influent raw water. By emphasizing particulate removal, multiple objectives are considered (e.g., organic removal, physical removal of pathogenic organisms, sorbed organic/inorganic removal, and turbidity reduction), which ultimately improves the effectiveness of microbial inactivation by disinfection and reduces the production of potentially carcinogenic disinfection by-products. To provide water of sufficient quantity and quality to consumers, the integrated design of the individual processes must be considered as the effluent of one process becomes the influent of the downstream process. The design process must also account for the desired flow capacity and influent water quality. Additionally, the US Environmental Protection

**TABLE 1** Individual treatment processes included in the three treatment configurations

| Configuration | Rapid Mix | Flocculation | Sedimentation | Filtration |
|---|---|---|---|---|
| Contact | X | | | X |
| Direct | X | X | | X |
| Conventional | X | X | X | X |

**TABLE 2** Water quality and flow rate parameter values used as inputs for determining the least-cost treatment regions

| Influent Parameter | Values |
|---|---|
| Particle concentration—*mg/L* | 1, 2, 3, 4, 6, 8, 12, 16, 24, 32, 48, 64, 80, 96, 112, 128 |
| Shape parameter—*d* | 2, 2.5, 3, 3.5, 4, 4.5, 5 |
| Size range—*µm* | 0.10–10.0, 0.25–25.0, 0.50–50.0, 0.75–75.0, 1.0–100.0 |
| Flow rate—*mgd (ML/d)* | 2 (7.57), 10 (37.85), 75 (283.88) |
| Particle density—*g/cm³* | 1.05, 1.20, 2.40 |
| Temperature—*°C* | 20 |

Agency (USEPA) requires a cost–benefit analysis when promulgating new regulations (Pontius, 1997), which further emphasizes the need to combine cost estimates, process models, and influent water quality conditions to enable representative national cost estimates to be generated for proposed regulatory actions (e.g., Frey et al, 1998; Gurian et al, 2001).

Early studies on particulate removal were focused on describing and exploring the effects of an integrated treatment system of rapid mix, flocculation, sedimentation, and filtration. Some of the earliest research to recognize the importance of describing particulate removal with an integrated design was developed by Gross et al (1978) and Lawler et al (1980) using different process models. Gross et al (1978) used a continuous formulation, assumed the influent particle diameters to be of one size, and performed an economic analysis of the sedimentation and filtration costs for treatment. Lawler et al (1980) assumed ideal plug-flow conditions, described the influent particle diameter distribution with a power law, and investigated a wider range of influent particulate and treatment characteristics. Ramaley et al (1981) furthered the study of Lawler et al (1980) by exploring the treatment behavior for two model waters with different particle densities and performing a sensitivity analysis on the treatment process parameters (mixing intensity, sedimentation residence time, and filter media size). These studies illustrate the complex behavior of particle removal and the need for an integrated design framework to make associated treatment decisions.

Wiesner (1985) and Wiesner et al (1987) followed the modeling approaches of Lawler et al (1980) and Ramaley et al (1981) to explore the least-cost design regions assuming charge neutralization conditions. These studies (Wiesner, 1985; Wiesner et al, 1987) used a simplified sedimentation model and optimal flocculation designs from the least-cost direct filtration solution as the basis for the conventional treatment design; thus, the decision process was not entirely integrated. Wiesner et al (1987) explored the behavior of contact, direct, and conventional treatment for seven influent particle characteristics and determined the least-cost design regions as a function of influent volume average diameter and concentration. Wiesner and Mazounie (1989) observed general agreement between actual treatment plant design and the regions predicted in Wiesner et al (1987). Wu and Ch... (1991) used empirical treatment process models and data from an existing treatment plant in a least-cost formulation that produced an optimal design close to that of the actual plant. Mhaisalkar et al (1993) solved the least-cost design problem using dynamic programming, assumed the influent particle characteristics were monodisperse and heterogeneous, and used simplified models to represent the flocculation and sedimentation processes. Mhaisalkar et al (1993) also performed a series of sensitivity analyses that showed the least-cost design and effluent concentration were not very sensitive to changes in the influent flow rate, suspended solids concentration, and treatment cost parameters. Dharmappa et al (1994) included a particle size distribution and process models similar to those of Lawler et al (1980) and Wiesner et al (1987) for flocculation and sedimentation, a modified filtration model based on O'Melia and Ali (1978), and incorporated waste-handling options in the treatment design. Their solution methodology investigated the least-cost design for three influent conditions.

The process models used by many researchers (Dharmappa et al, 1994; Wiesner et al, 1987; Wiesner, 1985; Ramaley et al, 1981; Lawler et al, 1980) to describe the changes in particle size distribution assume: (1) particles follow a rectilinear flow path (i.e., particle movement within a fluid is independent of hydraulic effects), and (2) all particles are spherical and nonporous. Studies by Han and Lawler (1991, 1992) presented a curvilinear modeling approach to account for hydrodynamic effects in the collision processes for nonporous, spherical particles. Additional studies have been undertaken to model the change in particle size distributions assuming porous particles that behave in a fractal nature (Lee et al, 2000; Li & Logan, 1997, 2000; Wiesner, 1992). Therefore, it could seem that the hard sphere rectilinear approach may be inadequate for representing particle behavior in actual treatment systems. Chellam and Wiesner (1993), ...

...ever, sugge... g., alum, ... approach ... nature of th... effects on t... -dimens... styrene sph... may be mo... ous, thus ... nally, the ... rectiline... gions that ... ant confi... may be app...

**OBJECTIVE...**

Much of ... developi... treatment p... considered ... cteristics a... ation of the ... ion of influ... volume ave... plete proces... influent con... achieve th... ect may no... stribution ... igurations. ... onfiguratio... ribution ra... ribution co... ics on the ... ather than ... ntage diam... ment plant ... tration d... nvestigate t... ion regio... en shown ... rticle den... fferent de... itions. Th... nsity valu... rganic p... presentati... ulate ma...

**...OCESS M...**

The curr... particle ... , sedim... proach ... wler et a... tion, trea...

suggest that for particles with fractal dimension ≤2 (e.g., clay-iron, kaolin [Wiesner, 1992]) the rectilinear approach may be suitable because of the relatively porous nature of the particles, which reduces the hydrodynamic effects on the particle movement. For particles with fractal dimensions ≥2.3 (e.g., ferric hydroxide floc, polystyrene spheres [Wiesner, 1992]) the curvilinear approach becomes more important as these particles are more impermeable, thus producing more hydrodynamic effects. Additionally, the study by Wiesner et al (1987), which used the rectilinear approach, resulted in least-cost treatment designs that were relatively consistent with actual treatment plant configurations indicating the rectilinear approach may be appropriate (Wiesner & Mazounie, 1989).

## OBJECTIVES

Much of the previous research has focused on modeling and developing a methodology for determining a least-cost treatment plant design. The work of Wiesner et al (1987) considered the widest range of influent particulate characteristics and was used to develop a qualitative representation of the least-cost treatment configurations as a function of influent particulate concentration and the influent volume average diameter. The current research uses comparable process models and significantly extends the range of influent conditions investigated by Wiesner et al (1987) to achieve three objectives. First, the volume average diameter may not be representative of the entire particle size distribution for determining the least-cost treatment configurations. Comparisons of the least-cost treatment plant configurations are made using both the particle size distribution range and shape of the influent particle size distribution to illustrate the importance of both characteristics on the resulting optimal treatment configurations (rather than the single, composite measure of the volume average diameter). Second, the design capacity of the treatment plant will affect the treatment cost and process configuration decisions. Three flow rates are considered to investigate the effect on the least-cost treatment configuration regions. Finally, the influent particle density has been shown to affect the treatment process behavior. Three particle densities are considered to investigate the effect different densities have on the least-cost treatment configurations. The range of densities considered include high-density values representative of water with predominantly inorganic particulate matter, and two low-density values representative of waters with predominantly organic particulate matter, such as humic acid.

## PROCESS MODELS

The current study focuses on describing the change in the particle size distribution through rapid mix, flocculation, sedimentation, and filtration using the rectilinear approach (Wiesner et al, 1987; Ramaley et al, 1981; Lawler et al, 1980) under nonsweep, or charge neutralization, treatment conditions. Particle destabilization under

**FIGURE 1** Optimal least-cost values for designs over a range of influent concentrations with an influent particle size range of 0.25–25 µm

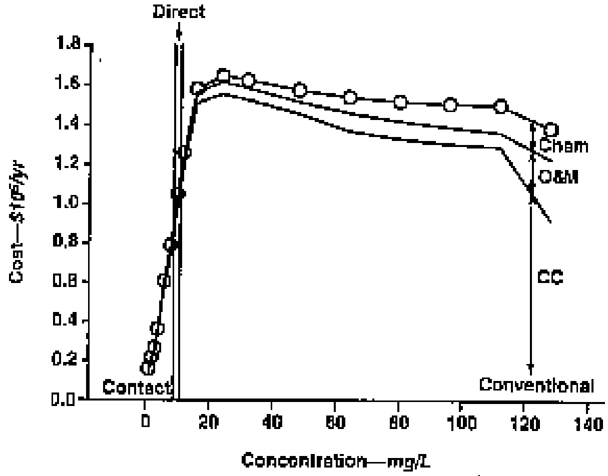


*The direct filtration region is the narrow region centered on 10 mg/L. The lines (without symbols) separate the total cost into capital costs (CC), operation and maintenance (O&M), and chemical (chem) costs (area between the lines). Total cost = CC annualized at 8% over 20 years + annual O&M cost + annual chem cost.*

charge neutralization conditions assumes the use of $6 \times 10^{-8}$ moles of cationic polymer addition per square metre (square foot) of particulate matter surface area (Wiesner et al, 1987). The influent particle size distribution can be described by a power law distribution (Lawler et al, 1980)

$$\frac{dN}{d\log(d_p)} = 2.3\, A d_p^{(1-\beta)} \qquad (1)$$

in which N is the number concentration of particles, $d_p$ is the particle diameter, $A$ is a parameter related to the particle concentration, and β is a parameter related to the shape of the particle size distribution. The particle size distribution is completely specified by selecting a value for β and the particle size range, which allows the determination of the volume average diameter, $(\overline{d_p})_V$. The continuous influent particle size distribution is represented by a logarithmic discretization of particle sizes into 51 discrete particle diameters using $\Delta\log(dp) = 0.04$ (as in Ramaley et al [1981], additional bins are included and initially left empty to account for the formation of particles with diameters up to 300 µm and prevent particle buildup in the largest influent particle size class). The change in particle size distribution through rapid mix, flocculation, and sedimentation is described using Smoluchowski's equations (Amirtharajah & O'Melia, 1990; Lawler et al, 1980). Removal of particles during sedimentation is incorporated using a term for Stokes' settling (Wiesner et al, 1987; Lawler et al, 1980) including a correction factor for drag on large particle sizes (Montgomery, 1985). The sedimentation tank is discretized into seven layers, which are coupled through the settling term. The particle collision efficiency, α, for the rapid mix, flocculation, and

**FIGURE 2** Least-cost design regions and cost contours as a function of the volume average diameter (with the associated β value provided) and influent particulate concentration for an influent particle range of 0.25–25 µm

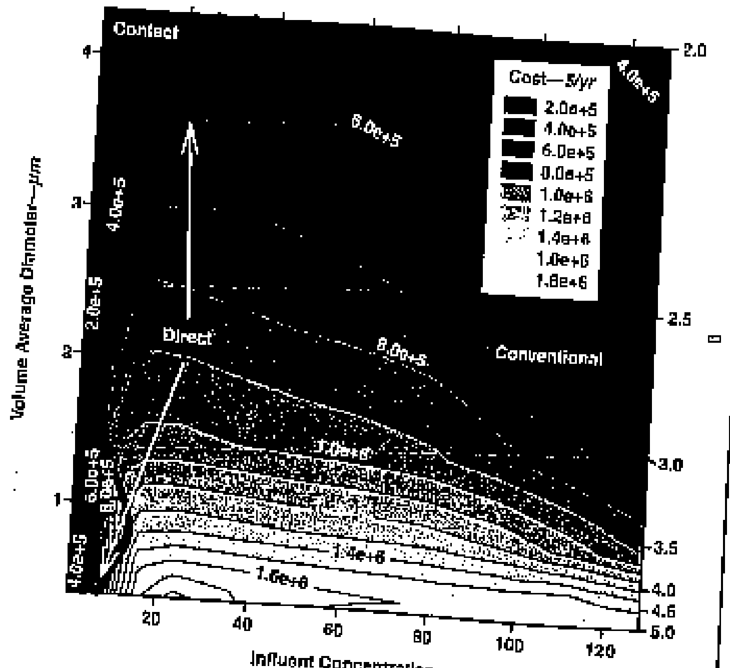


*Flow rate (Q) = 10 mgd (37.85 ML/d), ρ = 1.20 g/cm³*

sedimentation processes is set to 0.4 (Wiesner et al, 1987). The resulting set of ordinary differential equations (ODEs) (63–88 for rapid mix and flocculation and 441–616 for sedimentation, dependent on the influent size range) are a stiff set of ODEs solved using a Fortran solver[1] (Hindmarsh, 1983). The filtration model used was developed by O'Melia and Ali (1978) and uses the volume average diameter, $(\overline{d_p})_V$ (not the particle size distribution) and particulate concentration leaving the sedimentation tank, $C_f$, as inputs to the filter model. The filtration model assumes that the highest effluent concentration occurs immediately after the start of a filter run and that ripening causes continual filtration improvement. This assumption ignores the deterioration of effluent concentration from particulate breakthrough and, as a result, implicitly assumes that the maximum headloss is reached prior to the occurrence of particulate breakthrough. The filter media properties for this study consist of a media diameter, $d_m$, of 0.1 cm (0.04 in.) and a clean-bed porosity, ε, of 0.36. The collection efficiency of the sand media, $\alpha_f$, and entrapped particles, $\alpha_{f,p}$, are 0.76 and 0.08, respectively (Wiesner et al, 1987). The cost equations used to represent the capital costs and operating and maintenance (O&M) costs are taken from Clark (1982) and a modified form of the equations presented by Letterman (1980) to describe filtration O&M costs (Wiesner et al, 1987). Cationic polymer costs (not included in the Clark [1982] O&M costs) are included at $5,918/ton ($6.52/kg). The costs are updated to 1997 dollars and amortized over 20 years at an interest rate of 8%. Total cost is presented as the annualized capital cost, plus the annual O&M costs, plus the chemical costs. A complete description of the process models is provided in Boccelli (2003).

## PROBLEM FORMULATION

Three treatment configurations are considered for evaluating the least-cost design: contact, direct, and conventional filtration. Each configuration uses a combination of the individual treatment processes of rapid mix, flocculation, sedimentation, and filtration. Table 1 shows the individual treatment processes included in each of the treatment configurations. For each set of influent conditions considered, the least-cost design for each of the three treatment configurations is determined. The configuration with the lowest cost is then determined to be the least-cost option.

The cost and process models are incorporated into an optimization formulation to determine the least-cost treatment designs. The optimization problem is formulated as follows:

$$\min_{DV} \Sigma\, CC + \Sigma\, O\&M \qquad (2)$$

subject to individual process constraints

$$15 \le t_F \le 60 \text{ min} \qquad (3)$$

$$10 \le G_F \le 50 \text{ s}^{-1} \text{ (75 s}^{-1}\text{ for direct)} \qquad (4)$$

$$t_s \ge 0.5 \text{ h} \qquad (5)$$

$$6\ (0.15) \le L_f \le 480\ (12) \text{ L/min/m}^2 \text{ (gpm/sq ft)} \qquad (6)$$

and integrated process constraints

$$C_{eff} \le 0.6 \text{ mg/L} \qquad (7)$$

$$h_f \le 250 \text{ cm} \qquad (8)$$

$$0 \le RR \le 0.15 \qquad (9)$$

$$12 \le t_f \le 168 \text{ h} \qquad (10)$$

with the objective of minimizing the sum of the capital costs (CC) and operation and maintenance (O&M) costs by altering the appropriate decision variables subject to ind al and integrated process constraints. Ionic polymer costs (CC, O&M, and chemical) are not included in the optimization formulation because these costs, for any set of influent conditions (influent particle concentration, β, and others), are the same for contact, direct, and conventional treatment. Instead, the chemical costs are added after optimization without affecting the optimal solutions. There are four decision variables: flocculation tank volume, $V_F$ ($L^3$); mixing intensity, $G_F$ (time—$T^{-1}$); sedimentation, $A_s$; and filter area, $A_f$ ($L^2$) (all values are nonnegative). Preliminary results fixed four additional design parameters at optimal values such that the rapid mix volume was always selected to maintain a 0.1-s residence time with a mixing intensity of 700 $s^{-1}$; the sedimentation height was 5 m (16.41 ft); and the filter depth was 90 cm (35.43 in.) (Boccelli, 2003). The individual process constraints include flocculation residence time, $t_F = V_F/Q$ ($T$), and mixing intensity $G_F$ ($T^{-1}$); sedimentation residence time, $t_s = A_s h/Q$ ($T$); and filtration loading rate, $L_f = Q/A_f$ ($L^3/T/L^2$ [gpd/sq ft]) (Kawamura, 1991; Wiesner et al, 1987; Montgomery, 1985). The integrated constraints are implicitly functions of all the individual processes and are the reason the individual treatment processes must be considered simultaneously in the design process. Integrated constraints are provided on the effluent particulate concentration, $C_{eff}$, filter headloss, $h_f$, recycle ratio (the fraction of total flow used in the backwash process), RR; and filter run time, $t_f$. The effluent concentration constraint of 0.6 mg/L assumes 2.0 mg/L of particulate matter is equivalent to 1.0 ntu (Wiesner et al, 1987) and is based on the current regulation of 0.3 ntu. The effluent concentration, $C_{eff}$, is determined by averaging the effluent concentration values from $n_{filt}$ filters assuming staggered backwashing. For example, four filters with a run time of 40 h and staggered backwashing indicate one filter is backwashed every 10 h. Given the filtration model assumption, the maximum $C_{eff}$ occurs immediately after one filter completes a backwash cycle. Therefore, the $C_{eff}$ value of interest is the average of the effluent concentration from the filter that has just been backwashed and the effluent concentration from the three other filters that are 10, 20, and 30 h into their individual filter cycles. So, although the effluent concentration profile of an individual filter can exceed 0.3 ntu, the average of all filter effluents is constrained to not exceed 0.3 ntu. The number of filters designed is related to the flow rate by $n_{filt} = 1.2Q^{0.5}$, rounded up (Kawamura, 1991). The resulting problem is a nonlinear programming problem solved using a sequential quadratic programming algorithm (Biegler & Cuthrell, 1985). The resulting problem has four decision variables and 13 bounds and constraints for the conventional treatment problem.

**FIGURE 3** Least-cost design regions and filter loading rate contours as a function of the volume average diameter (with the associated β value provided) and influent particulate concentration for an influent particle range of 0.25–25 μm

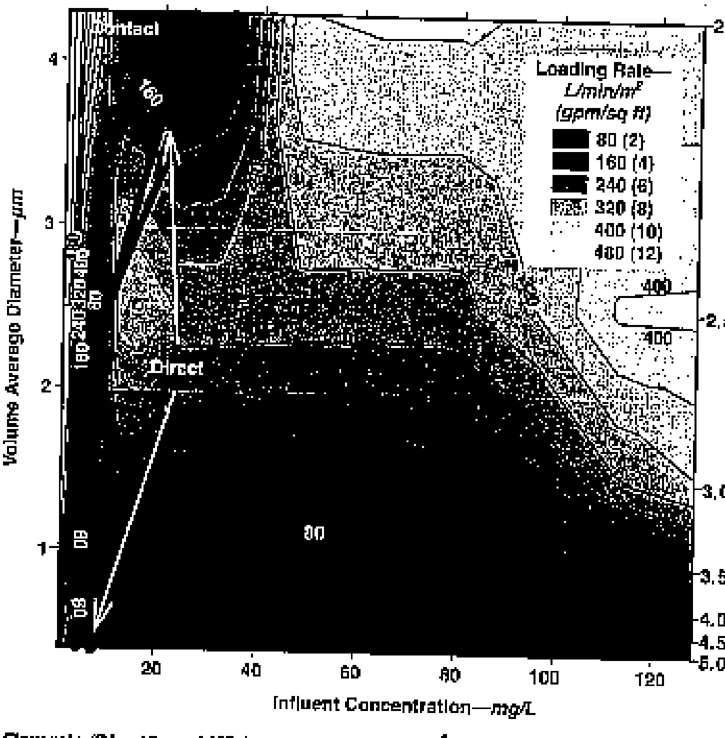


*Flow rate (Q) = 10 mgd (37.85 ML/d), ρ = 1.20 g/cm³*

Table 2 shows the extended initial conditions used to determine the least-cost design regions, based on the previous studies of Wiesner et al (1987) and Lawler et al (1980). The "base case" values in the first part of this study used a flow rate, $Q$, of 10 mgd (37.85 ML/d) and a particle density (ρ) of 1.20 g/cm³ (similar to Wiesner et al, 1987). To explore the effect of flow rate on the least-cost configurations, additional flow rates of 2 and 75 mgd (7.57 and 283.88 ML/d) were investigated with ρ = 1.20 g/cm³. To explore the effect of particle density on the least-cost configurations, additional density values of 1.05 and 2.40 g/cm³ were investigated with $Q$ = 10 mgd (37.85 ML/d). Sixteen influent particle concentrations, seven shape parameter values, β, and five particle size ranges were considered in developing the least-cost treatment configuration regions. Additional concentration and β values not presented in Table 2 were used where necessary to refine the graphical estimation of the least-cost configuration regions.

## RESULTS: BASE CASE

For the base case conditions of $Q$ = 10 mgd (37.85 ML/d) and ρ = 1.20 g/cm³, Figure 1 shows a typical least-

FIGURE 4 **Least-cost design regions and filter run time contours as a function of the volume average diameter (with the associated β value provided) and influent particulate concentration for an influent particle range of 0.25–25 µm**

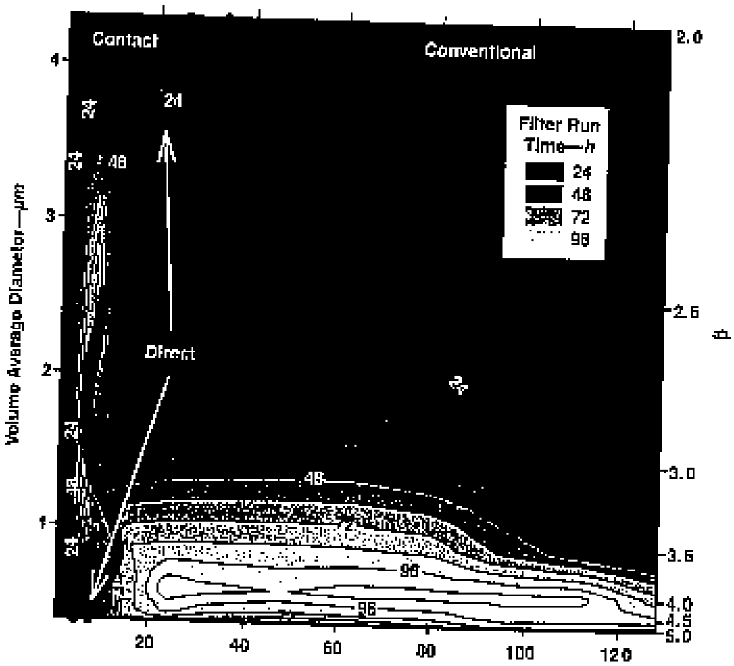


*Flow rate (Q) = 10 mgd [37.85 ML/d], ρ = 1.20 g/cm³*

cost curve over a range of influent particle concentrations with an influent particle size range of 0.25–25.0 µm and β = 4. Figure 1 shows the total treatment cost (line with symbols) and the fraction of the total cost because of capital (CC), O&M, and chemical (Chem) costs (area between lines). The maximum treatment cost typically occurs around an influent particulate concentration of 20–30 mg/L. The results in Figure 1 show the least-cost treatment configurations of contact, direct, and conventional treatment for the specified influent conditions. The direct filtration region, when present, is typically narrow. The rapid increase in cost at the low influent concentration values is usually associated with contact and direct filtration configurations. The costs continue to increase toward the maximum cost under conventional treatment because of the importance of the filtration process in these concentration regions (discussed further in the following section). The costs begin to decrease with increasing influent concentration as the sedimentation process becomes more important. A small portion of the annual costs are attributable to O&M (typically 3–6%), except at high influent concentrations (C = 128 mg/L), at which O&M accounts for about 22% of the annual costs because of an increase in flocculation mixing intensity. The chemical cost portion of the annual cost increases with influent concentration from 0.8 to 11% of the total annual cost.

**Least-cost configuration regions.** Figure 2 shows the optimal cost contours and least-cost treatment configurations over a range of influent concentrations and $(\overline{d_p})_V$ (with corresponding β values shown) for the base case conditions (Q = 10 mgd [37.85 ML/d]; ρ = 1.2 g/cm³) with an influent size range of 0.25–25 µm. The shape of the cost contours in Figure 2 are representative of the cost contours observed with the other four influent size regions. The cost of treatment tends to reach a maximum between β values of 4 and 4.5. The decrease in cost as β approaches a value of 5 is associated with the increase in particle number concentration in the small particle sizes. The increase in number concentration results in an increase in the collision frequency, so that treatment is easier and the cost of treatment is reduced. The cost contours for the other influent size regions are generally the same, particularly at larger influent sizes $(\overline{d_p})_V$ at which filter run time, not effluent concentration, primarily affects the design decisions.

Figure 2 also shows the least-cost configuration regions of contact, direct, and conventional treatment. Contact filtration is typically the least-cost configuration at low concentrations. The influent concentration at which contact filtration is the least-cost configuration increases with an increase in $(\overline{d_p})_V$, when $(\overline{d_p})_V$ is > 2 µm. Direct filtration is typically preferred only over a narrow range of influent concentration, though it is more likely to be optimal at low $(\overline{d_p})_V$ corresponding to high β values. For an influent particle size range of 0.25–25 µm, direct filtration is the least-cost treatment configuration in two small regions corresponding to the smaller and larger $(\overline{d_p})_V$ regions. Nonsweep conventional filtration is the predominant treatment configuration, with the largest ranges at very small particle diameters around $(\overline{d_p})_V$ of 1.5 µm.

When developing the least-cost designs, the constraint ranges for $L_f$ and $t_f$ were allowed to extend beyond typical design values to provide more possibilities in the optimal designs and to allow comparisons between design practice and the optimal results. Typical values for $L_f$ are 80 L/min/m² (2 gpm/sq ft) and above and for $t_f$ are 72 h or less. Figures 3 and 4 show the least-cost design regions and the associated values of $L_f$ and $t_f$, respectively, with an influent particle range of 0.25–25 µm. In general, there are two regions where the current design approach produces constraint values below the typical minimum loading rate or above the typical maximum run time: (1) as the influent concentration approaches the edge of the contact filtration regions and (2) for the conventional treatment region with $(\overline{d_p})_V \le 1$ µm (β between 3.5 and 5). If the constraints were adjusted to reflect typical design values, there could be a slight shift in the least-cost configuration boundary for $(\overline{d_p})_V$ around 2 µm, and this would certainly increase the design cost for conventional treatment for $(\overline{d_p})_V \le 1$ µm.

Figure 5 shows the least-cost design regions with an influent particle range of 0.25–25 µm and further separates the conventional treatment region into four regions (1A, 2A, 3A, 3B) based on the active constraints. For all constraint regions, the least-cost design results in an active headloss constraint of 250 cm (98.43 in.), which is a result of assuming no particulate breakthrough during the filter run time. Region 1A exists because of a rapid increase in design cost, and eventual infeasibility, of the direct filtration configuration while satisfying the RR constraint. The addition of sedimentation does not significantly affect particulate removal (sedimentation removes <2% of the particulate matter), yet enough particulate matter is removed to satisfy both the $C_{eff}$ and RR constraints. In region 2A, sedimentation removes significant particulate matter (>60%); however, the retention time and in most cases the mixing intensity in the flocculation basin are kept to a minimum. Therefore, under these influent particle size characteristics, creating larger particles does not appear to be an important consideration in the least-cost treatment of this region. Other than headloss, the only other active constraint is $C_{eff}$. Region 3A is the largest of the four regions and is where the flocculation retention time is generally at a maximum and sedimentation removes significant particulate matter; $C_{eff}$ remains the other active constraint. The last region is 3B (in the upper right quadrant of Figure 5), which is similar to 3A, except that both $C_{eff}$ and the minimum filter run time are active constraints. With the larger size ranges, as the volume average diameter continues to increase, the $C_{eff}$ constraint becomes less important to the point that the minimum filter run time constrains the problem, not the $C_{eff}$ constraint. When $(\overline{d_p})_V$ increases to such a large size, the cost differences between the various influent size ranges are small because the designs are not as heavily influenced by the need to satisfy the effluent concentration constraint.

The resulting treatment configuration and constraint regions can be related to the optimal filtration design. Figure 6 shows the fil-

**FIGURE 5** Least-cost design regions for contact, direct, and conventional treatment and constraint regions (1A, 2A, 3A, 3B) as a function of the volume average diameter (with the associated β value provided) and influent particulate concentration for an influent particle range of 0.25–25 µm

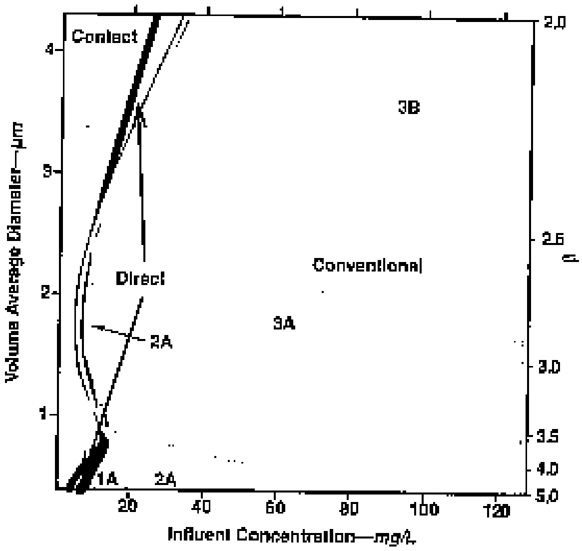


*1A—sedimentation included to satisfy the recycle ratio constraint, $C_{eff}$ constraint active; 2A—flocculation residence time and mixing intensity generally at a minimum, $C_{eff}$ constraint active; 3A—flocculation residence time at a maximum, $C_{eff}$ constraint active; 3B—$C_{eff}$ and minimum $t_f$ constraints active. Flow rate (Q) = 10 mgd [37.85 ML/d], ρ = 1.20 g/cm³*

**FIGURE 6** Cost of filtration as a function of the filter influent volume average diameter

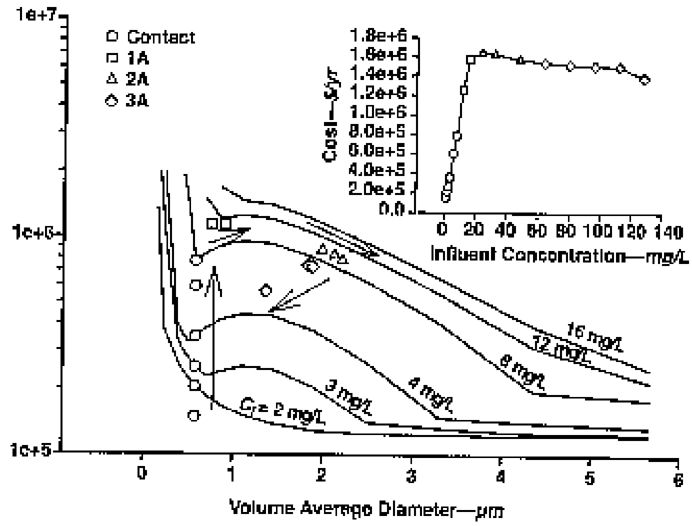


*Contours represent filtration costs for filter influent particulate concentrations, $C_I$; symbols represent the regions of contact and conventional treatment (for constraint regions 1A, 2A, 3A); arrows correspond to increasing plant influent particulate concentration (see inset, same as Figure 1). Influent size range of 0.25–25 µm and β = 4*

**FIGURE 7** Least-cost regions for the five influent concentration ranges shown as a function of the particle distribution shape parameter and the volume average diameter

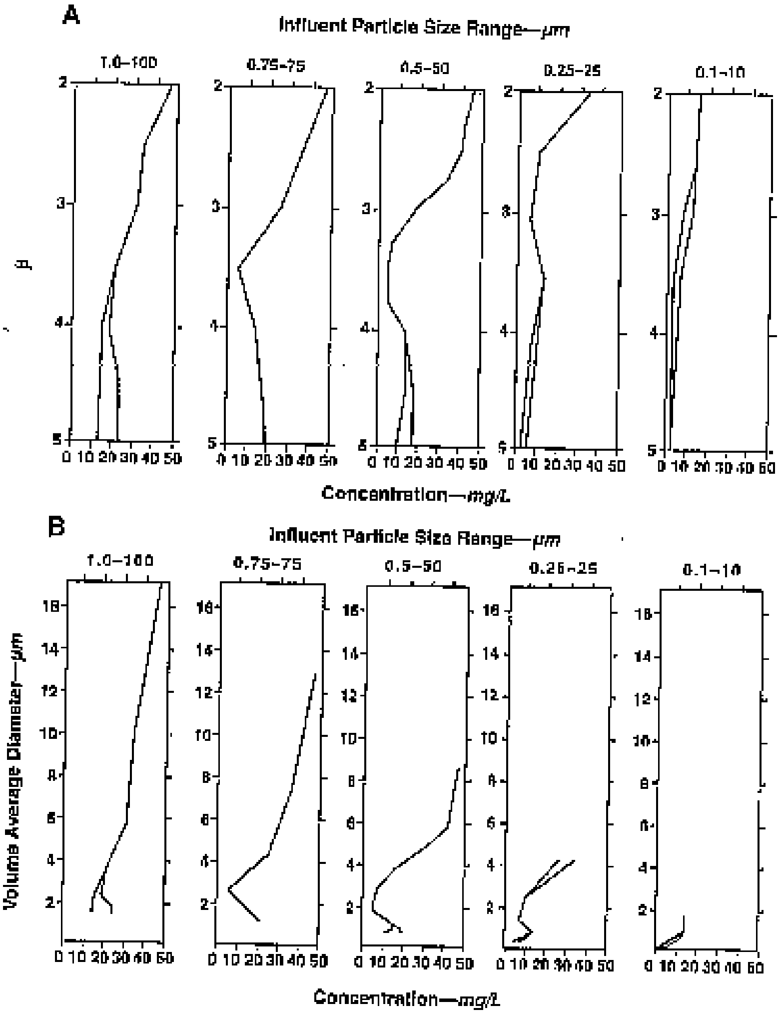


*Regions to the left of the lines are contact filtration, regions between the two lines are direct filtration, and regions to the right of the lines are conventional treatment.*

tration costs of the optimal designs for a given volume average diameter entering the filter, with contours representing the particle concentration entering the filter ($C_f$) not the plant. The inset in Figure 6 shows the total treatment cost against the influent particle concentration, and is the same as Figure 1. With the exception of the $C_f = 2$ mg/L contour, there is a rapid decrease in cost as $(\overline{d_p})_V$ increases, followed by a slight increase before the cost decreases again. The high cost at the small particle sizes is the result of the difficulty in satisfying the minimum filter run time ($C_f \leq 4$ mg/L) and RR ($C_f \geq 8$ mg/L) constraints. The maximum filter cost occurs near the particle size that is most difficult to remove (slightly > 1 µm) and corresponds to about the maximum total cost.

Figure 6 relates the constraint regions to the filtration design cost for an influent size range of 0.25–25 µm and β = 4. The arrows represent the filtration cost corresponding to an increase in plant influent particle concentration. Contact filtration is the least-cost option with a volume average diameter of 0.58 µm and an influent particulate concentration up to $C_f = 8$ mg/L (symbol = circle). During contact filtration, the cost simply increases with concentration. Within the conventional (1A) region (symbol = square), the $C_{eff}$ and RR constraints are active, and flocculation and sedimentation processes are added to satisfy the effluent and recycle constraints, not to create particles suitable for settling. In fact, the filter removes more than 98% of the particles from the water in this region. As the concentration increases into the conventional (2A) region (symbol = triangle) where the flocculation residence time is at a minimum, the filter is receiving a relatively constant influent concentration; however, $(\overline{d_p})_V$ is increasing. Further increases in the influent concentration move the solution into the 3A conventional region (symbol = diamond) where flocculation residence time is at a maximum, which results in smaller particles and lower influent concentrations entering the filter (sedimentation removes much of the larger particles and concentration). Overall, the changes in filtration cost mimic the changes in the total treatment cost. For the different influent size ranges and β values investigated, the treatment configurations and constraint regions are similarly related to the filtration design characteristics as in Figure 6.

In general, contact filtration is preferred until a hydraulic constraint (minimum filter run time or recycle ratio) either increases the cost rapidly or results in an infeasible design. At this point, direct filtration may be utilized to increase the particle size entering the filter. If direct filtration does not transition into the region where settleable particles are formed, sedimentation is added to assist in keeping a feasible design and has active constraints for both $C_{eff}$ and the RR. The regions where both the $C_{eff}$ and RR constraints are active generally only occur for concentrations <20 mg/L.

Although the least-cost design regions in Figure 2 are quantitatively different than those developed by Wiesner et al (1987), the regions are qualitatively similar in that contact filtration is the least-cost configuration at low influent particle concentrations, direct filtration only narrow region of least-cost configuration, and non-sweep conventional treatment is the dominant process configuration. The least-cost treatment curves also remain qualitatively similar, although the Wiesner et al (1987) study predicted a maximum treatment cost with an influent concentration of approximately 13 mg/L, in contrast to the maximum from this study at approximately 24 mg/L. Ultimately, this study illustrates the effect of changing particle size distribution characteristics, flow rate, and particle density on the least-cost configuration regions to demonstrate the need for considering these influent parameters and associated variabilities in the design process.

**Effect of shape parameter, β, and influent size range.** The least-cost design regions have been shown as a function of concentration and $(\overline{d_p})_V$ (Wiesner et al, 1987); however, both the range and shape of the particle size distribution influence the design selections. Figure 7 shows the least-cost treatment regions as functions of β (top) and $(\overline{d_p})_V$ (bottom). Although the various least-cost configuration regions have some similarities across the influent particle size regions, neither β nor $(\overline{d_p})_V$ completely determines the regions of least-cost treatment. That is, for a single value of $(\overline{d_p})_V$ or β, the least-cost treatment regions change with different influent particle size ranges. Therefore, generalizing design decisions based solely on β or $(\overline{d_p})_V$ may not be appropriate. In general, direct filtration is present as the least-cost treatment configuration at the lower $(\overline{d_p})_V$/higher β values. The exceptions to this are the results with an influent particle size range of 0.75–75 µm in which direct filtration is never the least-cost option and for an influent size range of 0.25–25 µm when there is an additional range of direct filtration at higher $(\overline{d_p})_V$/lower β. Conventional treatment has the largest range of least-cost treatment configuration at small $(\overline{d_p})_V$ (< 0.5 µm) and for $(\overline{d_p})_V$ between 1 and 3 µm. Larger influent $(\overline{d_p})_V$ reduces the range of conventional treatment as the least-cost option.

Figure 8 presents the treatment cost for C = 4, 32, and 128 mg/L for $(\overline{d_p})_V$ corresponding to the five particle size ranges with β = 2, 3, 4, and 5. For an influent concentration of 4 mg/L (top), the cost curves are the same over the range of influent $(\overline{d_p})_V$ for the five influent particle size ranges considered. This is not surprising because these solutions are all within the contact filtration range, which is only dependent on $(\overline{d_p})_V$ (there are no other processes to alter the particle size distribution). As the influent concentration increases from 32 mg/L (middle) to 128 mg/L (bottom), the costs are essentially the same (in a conventional treatment region) for the larger influent $(\overline{d_p})_V$, whereas at the smaller influent $(\overline{d_p})_V$, the particle range has an effect on the design cost—not just the influent volume average diameter. This further illustrates that $(\overline{d_p})_V$ may not be appropriate as the sole parameter for basing design decisions.

## RESULTS: EFFECT OF FLOW RATE

Treatment plant designs will vary from location to location and be designed for a variety of flow capacities. Fig-

**FIGURE 8** Least-cost treatment curves for three influent particle concentrations (*C*) and influent volume average diameters associated with five influent particle size ranges and β = 2, 3, 4, and 5

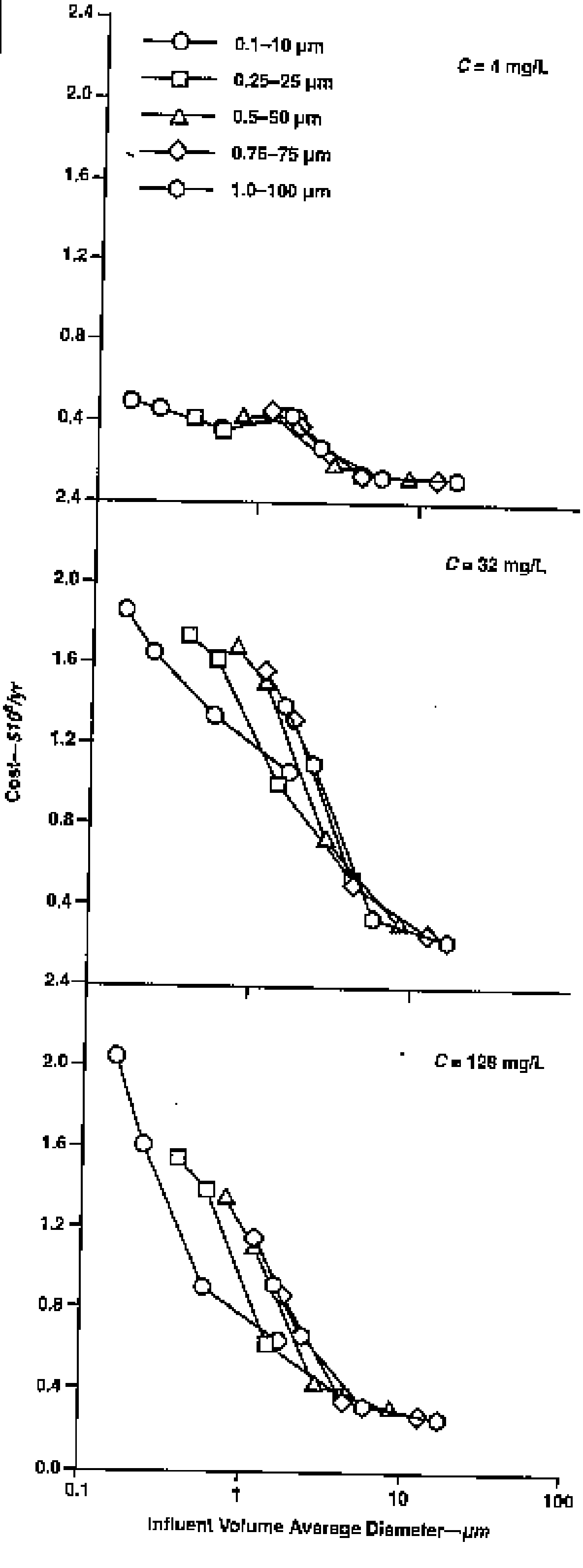

FIGURE 9 Least-cost regions as a function of influent $(\overline{d_p})_V$ and particulate concentration for three flow rates

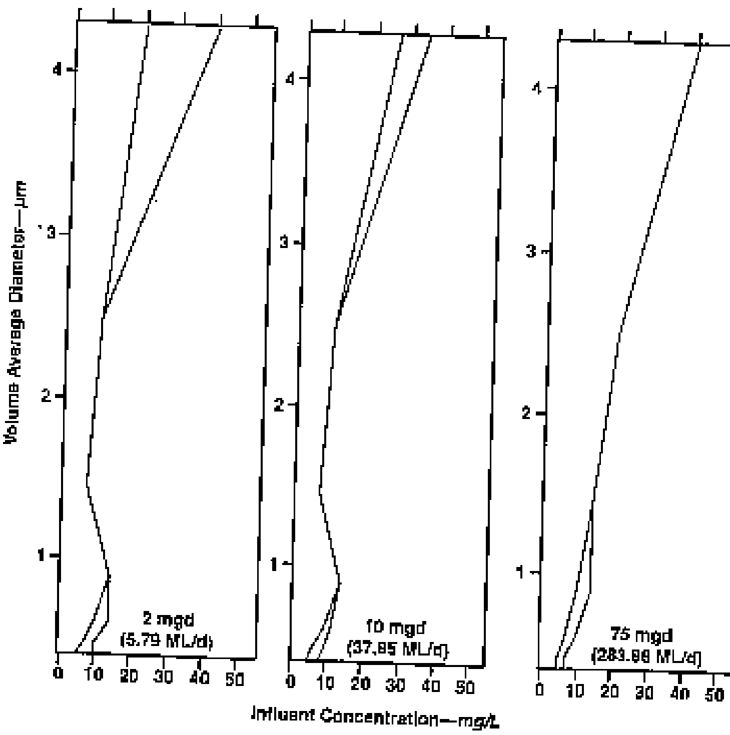


*Regions to the left of the lines are contact filtration, regions between the two lines are direct filtration, and regions to the right of the lines are conventional treatment. Influent particle diameter range = 0.25–25 μm*

ure 9 shows the least-cost treatment configuration regions for three design flow rates of 2, 10, and 75 mgd (7.57, 37.85, and 283.88 ML/d) for an influent particle size range of 0.25–25 μm. For $Q$ = 2 and 10 mgd (7.57 and 37.85 ML/d), there are two distinct regions in which direct filtration is the least-cost treatment configuration versus one region when $Q$ = 75 mgd (283.88 ML/d). The direct filtration region for $(\overline{d_p})_V \geq 2.5$ μm is the largest when $Q$ = 2 mgd (7.57 ML/d) and disappears completely when $Q$ = 75 mgd (37.85 ML/d). For the direct filtration region at smaller $(\overline{d_p})_V$, increasing $Q$ increases the particle size range in which direct filtration is the least-cost treatment configuration. For the direct filtration region at larger $(\overline{d_p})_V$, increasing $Q$ decreases the direct filtration region, and the contact filtration region expands to make up the difference. For $(\overline{d_p})_V$ between 1.25 and 2.5 μm, increasing $Q$ also expands the region of contact filtration.

In general, increasing $Q$ results in an increase in the treatment plant design cost. This is simply because of the increase in treatment process capacity necessary to accommodate the additional flow rate. The treatment plant cost per unit of flow rate, however, does not necessarily increase with $Q$. Figure 10 illustrates the economies of scale associated with the least-cost designs for the different $Q$ values over a range of influent concentrations and an influent particle size range of 0.25–25 μm and β = 4 by normalizing the annual cost by the flow rate in million gallons per day (megalitres per day). The least-cost design profile for the normalized cost with $Q$ = 2, 10, and 75 mgd (7.57, 37.85, and 283.88 ML/d) maintains the same relative shape as the annual cost in Figure 1. The maximum treatment cost remains at influent particulate concentrations between 20 and 30 mg/L, and larger plants produce water at lower cost per 1,000 gal (3,785 L) than smaller plants, thus achieving economies of scale.

## RESULTS: EFFECT OF PARTICLE DENSITY

Figure 11 shows changes in the least-cost configuration regions with respect to changes in particle density. For the smaller and larger $(\overline{d_p})_V$ ranges, increasing ρ decreases the regions where direct filtration is the least-cost treatment configuration. For the larger $(\overline{d_p})_V$ region, the direct filtration region completely disappears with the increased particle density. For the smaller $(\overline{d_p})_V$ region, increases in particle density tend to shift the direct filtration region to low $(\overline{d_p})_V$ values.

As particle density increases, the region of conventional treatment actually decreases with larger particle sizes where sedimentation becomes more efficient in removing larger particulate matter (Figure 11). Figure 11 shows that increasing the particle density to 2.40 g/cm³ actually reduces the amount of particulate matter

FIGURE 10 Cost per 1,000 gal of water for increasing flow rates over a range of influent concentrations

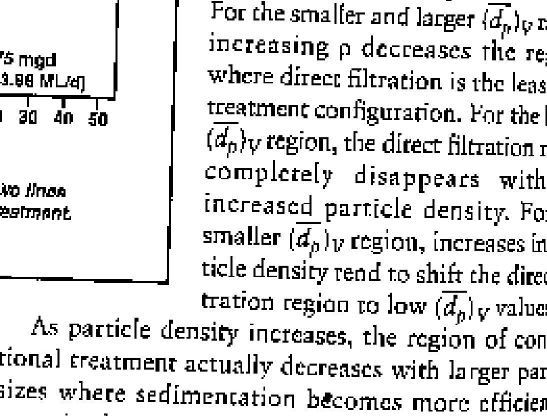


*Influent size range of 0.25–25 μm, β = 4, Q—flow rate*

**TABLE 3 Individual and integrated process constraint values from the optimal designs of contact filtration with $C = 4$ mg/L, conventional filtration with $C = 48$ mg/L, and $\beta = 3$ and 4 for various influent particle size ranges, particle densities, and flow rates**

| Configuration | β | $(\overline{d_p})_V$ µm | $t_F$ min | $G_F$ $s^{-1}$ | $t_s$ h | $L_f$—L/min/m² (gpm/sq ft) | $C_{eff}$ mg/L | RR % | $t_f$ h |
|---|---|---|---|---|---|---|---|---|---|
| Influent size range 0.25–25.0 µm, ρ = 1.2 g/cm³, Q = 10 mgd (37.85 ML/d) | | | | | | | | | |
| Contact | 3.0 | 1.46 | | | | 74.0 (1.85) | 0.60 | 3.0 | 62.2 |
| Contact | 4.0 | 0.60 | | | | 109 (2.72) | 0.60 | 8.5 | 12.0 |
| Conventional | 3.0 | 1.46 | 60.0 | 35.5 | 19.4 | 128 (3.20) | 0.60 | 2.9 | 37.9 |
| Conventional | 4.0 | 0.60 | 15.0 | 10.0 | 31.6 | 30.9 (0.77) | 0.60 | 4.3 | 107 |
| Influent size range 0.75–75.0 µm, ρ = 1.2 g/cm³, Q = 10 mgd (37.85 ML/d) | | | | | | | | | |
| Contact | 3.0 | 4.37 | | | | 413 (10.3) | 0.36 | 2.8 | 12.0 |
| Contact | 4.0 | 1.80 | | | | 90.5 (2.26) | 0.60 | 2.6 | 58.5 |
| Conventional | 3.0 | 4.37 | 60.0 | 34.5 | 5.10 | 309 (7.72) | 0.60 | 2.8 | 15.9 |
| Conventional | 4.0 | 1.80 | 60.0 | 36.1 | 12.0 | 32.5 (0.81) | 0.60 | 4.0 | 109 |
| Influent size range 0.75–75.0 µm, ρ = 1.2 g/cm³, Q = 75 mgd (283.88 ML/d) | | | | | | | | | |
| Contact | 3.0 | 4.37 | | | | 414 (10.3) | 0.17 | 2.8 | 12.0 |
| Contact | 4.0 | 1.80 | | | | 306 (7.65) | 0.46 | 3.8 | 12.0 |
| Conventional | 3.0 | 4.37 | 15.0 | 20.2 | 2.73 | 198 (4.95) | 0.46 | 6.1 | 12.0 |
| Conventional | 4.0 | 1.80 | 60.0 | 32.9 | 9.91 | 112 (2.80) | 0.60 | 5.8 | 22.0 |
| Influent size range 0.75–75.0 µm, ρ = 2.4 g/cm³, Q = 10 mgd (37.85 ML/d) | | | | | | | | | |
| Contact | 3.0 | 4.37 | | | | 480 (12.0) | 0.14 | 1.9 | 14.9 |
| Contact | 4.0 | 1.80 | | | | 269 (6.72) | 0.60 | 2.2 | 23.1 |
| Conventional | 3.0 | 4.37 | 15.0 | 10.0 | 1.14 | 303 (7.57) | 0.57 | 3.9 | 12.0 |
| Conventional | 4.0 | 1.80 | 60.0 | 24.1 | 1.07 | 59.5 (1.49) | 0.60 | 9.1 | 27.4 |

$A_f$—filter area, β—a parameter related to the shape of the particle size distribution, $C$—concentration, $C_{eff}$—effluent particulate concentration, $d_p$—particle diameter, $(\overline{d_p})_V$—volume average diameter, $G_F$—mixing intensity, $L_f$—filtration loading rate ($Q/A_f$), ρ—particle density, Q—flow rate, RR—recycle ratio, $t_f$—filter run time, $t_F$—flocculation residence time ($V_F/Q$), $t_s$—sedimentation residence time, $V_F$—flocculation tank volume

removed in the sedimentation tank for β = 4 and size ranges of 0.25–25 µm and 0.75–75 µm. This effect is greater for the larger particle ranges (which translate to a larger range of $(\overline{d_p})_V$ values). Instead, the primary-removal process is shifted to the filters. This occurs for a few reasons. First, for a given concentration, the particle number concentration is less when the particle density is higher; thus, fewer collisions occur, reducing the number of larger particles formed (which is suppressed by a general reduction in the flocculation volume retention time). Second, with higher-density particles, larger particles are removed faster, which decreases the concentration and residence time of larger particles to further remove smaller particles through differential sedimentation; thus, the less-settleable, smaller particles are left behind for removal by the filters. This behavior of quickly removing the largest particles for a dense suspension, leaving poorly settleable particles behind, was also observed by Ramaley et al (1981). Finally, increasing the particle density improves the filter removal efficiency of particles greater than 1 µm in diameter. Therefore, the presence of more-dense particles does not necessarily mean that sedimentation will become the more important removal process. In general, for smaller $(\overline{d_p})$, the sedimentation volume tends to be much smaller for more-dense particles and the filter area much larger.

## RESULTS: OPTIMAL DESIGNS

Table 3 provides the individual and integrated process constraint values for contact filtration with C = 4 mg/L and conventional filtration with C = 48 mg/L over a range of influent conditions. As previously discussed, all of the optimal designs have $h_f$ = 250 cm (98.43 in.). The first set of results is representative of the "base case" solutions (particle size range of 0.25–25 µm, ρ = 1.20 g/cm³, and Q = 10 mgd [37.85 ML/d]). For contact filtration, β = 3 results in a lower loading rate because the associated $(\overline{d_p})_V$ is closer to the particle diameter associated with minimum filter efficiency (about 1–2 µm). For conventional treatment, β = 3 is in the 3A constraint region (maximum flocculation), whereas for β = 4 the solution is in the 2A constraint region (minimum flocculation). In both cases, the optimal settling time is large, and these

FIGURE 11 Least-cost regions as a function of influent $(\overline{d_p})_V$ and particulate concentration for three particle densities

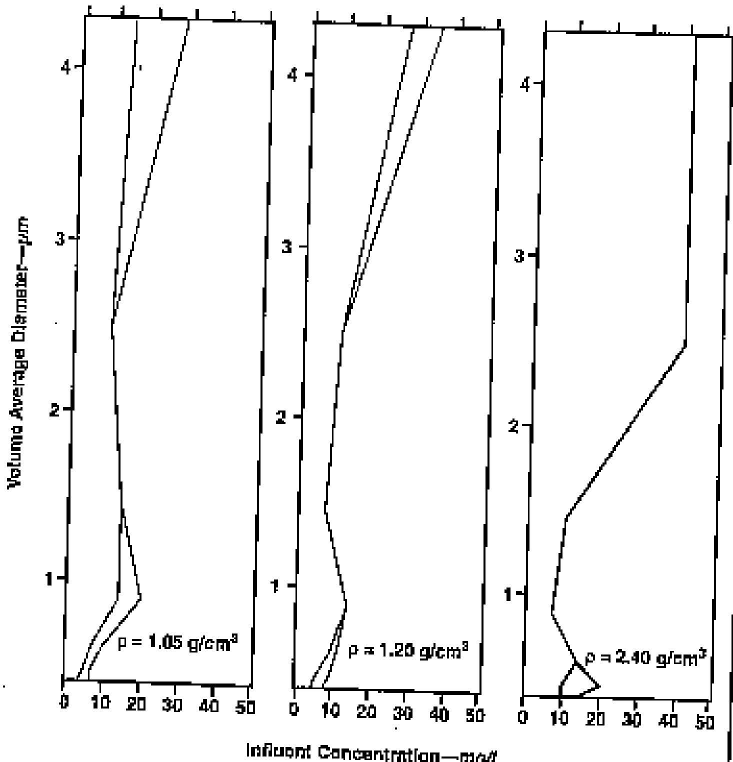


*Regions to the left of the lines are contact filtration, regions between the two lines are direct filtration, and regions to the right of the lines are conventional treatment. Influent particle diameter range = 0.25–25 µm*

influent conditions may be better treated by alternative process configurations (such as sweep–floc conventional treatment). The second set of results illustrates the effect of a larger influent particle size range of 0.75–75 µm. For contact filtration, $\beta = 3$ corresponds to a higher filtration rate because the associated $(\overline{d_p})_V$ is much larger than the particle diameter associated with minimum filter efficiency. The solution with $\beta = 3$ is also constrained by the minimum filter run time, not the effluent concentration. For conventional treatment, both solutions are in the 3A constraint region and have a significant reduction in the optimal settling time. This indicates that the larger influent particle size range is more amenable to non-sweep conventional filtration. The third set of results shows the optimal constraints for the highest flow rate, $Q = 75$ mgd (283.88 ML/d). Both contact filtration solutions are constrained by the minimum filter run time, not the effluent concentration, and have high loading rates. For the conventional solutions, the cost associated with designing larger individual processes shifts the particulate removal from the sedimentation tank to filtration, which translates to a decrease in the settling time. For $\beta = 3$, the constraint solution is similar to the 2A region except that the filter run time, not the effluent concentration, is active for this solution. The final set of results is for the high-density particles $\rho = 2.40$ g/cm³ and mid-range flow rate, $Q = 10$ mgd (37.85 ML/d). For contact filtration, $\beta = 3$ results in the maximum allowable loading rate, whereas $\beta = 4$ simply increases the loading rate. For conventional filtration and in line with Figure 12, the particulate removal is shifted to the filters with an associated reduction in the optimal settling time.

## DISCUSSION

The integrated design of a drinking water treatment plant is important when exploring the cost-effective options for satisfying the hydraulic and effluent concentration constraints. Although this study investigates a wide range of influent conditions and considers three treatment configurations, additional factors or treatment options may affect the design decisions. First, this work only considers particulate removal, whereas the actual design of a treatment plant must also consider the treatment of multiple organic, inorganic, and microbial components. This includes natural organic matter (NOM) removal and should consider the impact of NOM on disinfectant by-product formation within the treatment plant as well as in the distribution system. Second, variations in raw water conditions must be considered because of the inherent variability in the influent water quality and quantity. The current study illustrates that variations in particle size distribution characteristics, flow rate, and particle density can affect the design cost and treatment options, and these variations should be considered during the design process. Additionally, the uncertainty in specifying the correct polymer dose to provide particle destabilization via charge neutralization also needs to be considered. Third, additional treatment options may be available to treat some of the influent water quality ranges evaluated and handle additional contaminant species. For example, sweep–floc conventional treatment would most likely be a competitive-cost alternative to nonsweep–floc conventional treatment for the low-density particulate matter waters that resulted in the most expensive treatment. In such cases, the additional particles created by coagulant addition improve the processes of flocculation and sedimentation for removing the existing particles. Finally, waste-handling streams can add significant cost to the treatment plant design (Dharmappa et al [1994] state that the waste-handling costs can be 30–50% of the total plant costs). In the sweep–floc conventional treatment option, the treatment processes may be less expensive relative to the non-sweep–floc conventional treatment option; however, the addition of more solids to the waste stream will affect the overall cost. These are just some of the issues that mi[...]

...dered when estimating total treatment cost, further emphasizing the need for integrated treatment plant design.

## SUMMARY

The removal of particulate matter during drinking water treatment is a complex process that is affected by the influent particle concentration and size distribution. When considering various treatment plant configurations, an integrated design framework must be considered during the design process rather than designing on an individual-process basis without regard for the interactions between processes. Such a process-by-process design can yield a configuration that does not adequately satisfy the treatment objectives. With such complex processes and the consideration of process cost, formulating the problem as a mathematical optimization problem provides the design engineer with a tool to efficiently evaluate a range of possible designs that minimize cost and satisfy the system constraints.

The base case results ($Q$ = 10 mgd [37.85 ML/d], $\rho$ = 1.05 g/cm$^3$) illustrate that the maximum treatment cost typically occurs in the range of 20–30 mg/L and for influent particle size distributions with shape values of $\beta$ between 4.0 and 4.5 (smaller-diameter particles). Treatment costs decrease with an increase in large-particle number concentration in the size distribution and with higher-particulate-concentration waters. The overall treatment costs mimic the filtration costs, increasing up to influent concentrations of about 20–30 mg/L and decreasing thereafter. Nonsweep–floc conventional filtration is the predominant treatment configuration specified. Contact filtration is the least-cost option for lower-influent-particulate concentrations, and direct filtration—when present—has narrow regions as the least-cost configuration, predominantly at smaller $(\overline{d_p})_V$ values. There are some regions in which nonsweep–floc conventional treatment is specified at smaller $(\overline{d_p})_V$, when the sedimentation tank is added to satisfy the effluent concentration and RR constraints, rather than serving as the primary removal process (<2% of particles are removed by sedimentation under this scenario). The results from the base case study also illustrate that although the $(\overline{d_p})_V$ may be a convenient measure for illustrating trends in treatment, its value does not uniquely determine the preferred treatment configurations across different particle size ranges. Both the particle size distribution shape and range, which together specify the value of $(\overline{d_p})_V$, are needed to determine the least-cost treatment configuration regions.

Treatment plant designs are site-specific, and will differ based on the desired capacity and raw water characteristics to be treated. Therefore, the effects of different flow rates and particle densities are evaluated with respect to the least-cost treatment configuration regions. Increasing the flow rate ($Q$ = 2, 10, and 75 mgd [7.57, 37.85, and 283.88 ML/d]) reduces the region of direct filtration at larger $(\overline{d_p})_V$ and expands the region of direct filtration at smaller $(\overline{d_p})_V$. In general, increasing the flow rate expands the region in which contact filtration is optimal. Although increasing the flow rate increases the overall design cost, the cost per gallon decreases, illustrating economies of scale for higher-capacity plants. Increasing particle density ($\rho$ = 1.05, 1.20, and 2.40 g/cm$^3$) decreases the direct filtration regions and expands the contact filtration regions as the least-cost treatment configurations. Although increasing $\rho$ reduces the cost of treatment by reducing the size of the sedimentation tank because of more efficient removal of large particles during sedimentation, the actual percentage of particulate matter removed by the sedimentation tank decreases with increasing particle density. The reduction in particulate removal during sedimentation comes as a result of better large-particle removal, which would otherwise continue to flocculate with smaller particles via differential sedimentation, thus decreasing the overall removal of particulate matter from the water.

**FIGURE 12** Fraction of particulate matter removed by the filter for different particle densities over a range of influent concentrations for two influent size ranges

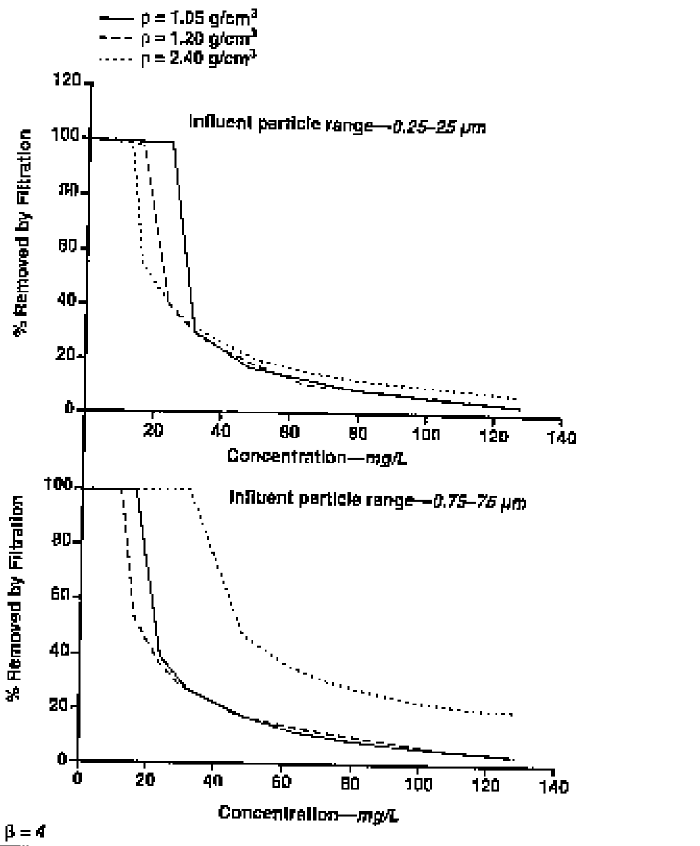



## ACKNOWLEDGMENT

This research was performed while Boccelli was a doctoral student in the Department of Civil and Environmental Engineering at Carnegie Mellon University. The authors acknowledge the National Science Foundation

ABOUT THE AUTHORS

*Dominic L. Boccelli[2] is a postdoctoral Oak Ridge Institute for Science and Education research participant at the Centers for Disease Control and Prevention and the University of Cincinnati, Department of Civil and Environmental Engineering, POB 210071, Cincinnati, OH 45221-0071; (513) 368-7652; e-mail dominic.bocelli@uc.edu. Boccelli has undergraduate degrees in chemistry and environmental engineering from*

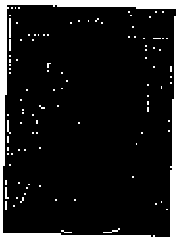

*Water Resources Planning and Management. Mitchell J. Small is the H. John Heinz III Professor of Environmental Engineering at Carnegie Mellon University. Urmila M. Diwekar is a professor in the Department of Chemical Engineering and the Institute for Environmental Science and Policy at the University of Illinois, Chicago.*

## FOOTNOTES

[1]Livermore Solver for Ordinary Differential Equations (LSODE), for Applied Scientific Computing, Lawrence Livermore National Laboratory, Livermore, Calif.

[2]To whom comments should be addressed

## REFERENCES

Amirtharajah, A. & O'Melia, C.R., 1990. Coagulation Processes: Destabilization, Mixing, and Flocculation. *Water Quality and Treatment*, McGraw-Hill, N.Y.

Biegler, L.T. & Cuthrell, J.E., 1985. Improved Infeasible Path Optimization for Sequential Modular Simulators II: The Optimization Algorithm. *Computers & Chem. Engrg.*, 9:3:257.

Boccelli, D.L., 2003. A Decision Support Tool for the Design of Integrated Treatment Systems for Drinking Water Utilities. Doctoral thesis, Carnegie Mellon University, Pittsburgh, Pa.

Chellam, S. & Wiesner, M.R., 1993. Research Note: Fluid Mechanics and Fractal Aggregates. *Water Res.*, 27:9,1493.

Clark, R.M., 1982. Cost Estimating for Conventional Water Treatment. *Jour. Envir. Engrg.—ASCE*, 108:EE5:819.

Dharmappa, H.B. et al, 1994. Water-Treatment System-Design for Turbidity Removal II: Optimization. *Jour. Envir. Engrg.—ASCE*, 120:4:921.

Frey, M.M. et al, 1998. Cost to Utilities of a Lower MCL for Arsenic. *Jour. AWWA*, 90:3:89.

Gross, D.C.; FitzPatrick, J.A.; & Gemmell, R.S., 1978. A Systems Analysis of the Solid–Liquid Separation Processes of a Water Treatment Plant. Proc. 1978 Ann. Conf. AWWA.

Gurian, P.L. et al, 2001. Benefit–Cost Estimation for Alternative Drinking Water Maximum Contaminant Levels. *Water Res.*, 37:8:2213.

Han, M. & Lawler, D.F., 1992. The (Relative) Insignificance of G in Flocculation. *Jour. AWWA*, 84:10:79.

Han, M. & Lawler, D.F., 1991. Interactions of Two Settling Spheres: Settling Rates and Collision Efficiency. *Jour. Hydr. Engrg.—ASCE*, 117:10:1269.

Hindmarsh, A.C., 1983. A Systematized Collection of ODE Solvers (R.S. Stepleman, editor). *Scientific Computing: Applications of Mathematics and Computing to the Physical Sciences*. Amsterdam, North, the Netherlands.

Kawamura, S., 1991. *Integrated Design of Water Treatment Facilities*. John Wiley & Sons, N.Y.

Lawler, D.L.; O'Melia, C.R.; & Tobiason, J.E., 1980. Integral Water Treatment Plant Design: From Particle Size to Plant Performance (M.C. Kavanaugh & J.O. Leckie, editors). *Particulates in Water: Characterization, Fate, Effects, and Removal*. Adv. in Chemistry series, 189. ASCE, Washington.

Lee, D.G. et al, 2000. Modeling Coagulation Kinetics Incorporating Fractal Theories: A Fractal Rectilinear Approach. *Water Res.*, 34:7:1987.

Letterman, R.D., 1980. Economic Analysis of Granular-bed Filtration. *Jour. Envir. Engrg.—ASCE*, 106:EE2:279.

Li, X.Y. & Logan, B.E., 2000. Settling and Coagulating Behavior of Fractal Aggregates. *Water Sci. & Technol.*, 42:3:253.

Li, X.Y. & Logan, B.E., 1997. Collision Frequencies of Fractal Aggregates With Small Particles by Differential Sedimentation. *Envir. Sci. & Technol.*, 31:4:1229.

Mhaisalkar, V.A. et al, 1993. Dynamic Programming Optimization of Water Treatment Plant Design. *Jour. Envir. Engrg.—ASCE*, 119:6:1158.

Montgomery, J.M., 1985. *Water Treatment Principles and Design*. James M. Montgomery, Consulting Engineers, Wiley Interscience, N.Y.

O'Melia, C.R. & Ali, W., 1978. The Role of Retained Particles in Deep-bed Filtration. *Prog. Water Technol.*, 10:5:167.

Pontius, F.W., 1997. Future Directions in Water Quality Regulations. *Jour. AWWA*, 89:3:40.

Ramaley, B.L. et al, 1981. Integral Analysis of Water Plant Performance. *Jour. Envir. Engrg.—ASCE*, 107:EE3:547.

Wiesner, M.R., 1992. Kinetics of Aggregate Formation in Rapid Mix. *Water Res.*, 26:3:379.

Wiesner, M.R., 1985. Optimal Water Treatment Plant Configuration: Effects of Raw Water Characteristics. Doctoral thesis, Johns Hopkins University, Baltimore.

Wiesner, M.R. & Mazounie, P., 1989. Raw Water Characteristics and the Selection of Treatment Configurations for Particulate Removal. *Jour. AWWA*, [illegible]

Wiesner, M.R.; O'Melia, C.R.; [illegible] 1987. Optimal Water Treatment Plant Design. *Jour. Envir. Engrg.*, 113:3:567.

Wu, M.Y. & Chu, W.S., 1991. Systems [illegible] of Water Treatment Plant [illegible] *Water Resources Planning and Management*, 117:5:536.